ISSN 0965-5425, Computational Mathematics and Mathematical Physics, 2020, Vol. 60, No. 4, pp. 737–748. © Pleiades Publishing, Ltd., 2020.
Russian Text © The Author(s), 2020, published in Zhurnal Vychislitel'noi Matematiki i Matematicheskoi Fiziki, 2020, Vol. 60, No. 4, pp. 752–764.

Dedicated to Academician S.K. Godunov on the occasion of his 90th birthday

Application of the Nesvetay Code for Solving Three-Dimensional High-Altitude Aerodynamics Problems

V. A. Titarev[a,*]

[a] *Federal Research Center "Computer Science and Control," Russian Academy of Sciences, Moscow, 119333 Russia*

**e-mail: titarev@ccas.ru, titarev@mail.ru*

Received October 21, 2019; revised October 21, 2019; accepted December 16, 2019

Abstract—A survey of the capabilities of the Nesvetay code as applied to computing the flow of a high-speed monatomic gas around objects of irregular shape for large flight altitudes is given. An implicit numerical method on an arbitrary unstructured grid and a two-level approach to the organization of parallel computations are described. This code is compared with the well-known MONACO and SMILE codes that implement the direct simulation Monte Carlo method.

Keywords: kinetic equation, S-model, rarefied gas, computational aerodynamics, unstructured mesh, supercomputer computations

DOI: 10.1134/S0965542520040168

INTRODUCTION

In recent years, due to the rapid development of numerical methods and increased performance of supercomputers, methods of the simulation of 3D rarefied gas dynamics based on the direct numerical solution of the kinetic Boltzmann equation with the exact or model collision integral have gained popularity. An attractive feature of this approach is that it makes it possible to develop efficient Godunov-like [1] second-order methods that can be used both for steady and unsteady flows. The corresponding software packages are developed by various groups of researchers (e.g., see [2–6]). The ability of using kinetic equations with approximate (model) collision operators [7–9] seems especially attractive for solving complicated applied (industrial) problems. Methods for solving model equations are highly efficient and flexible, and have acceptable accuracy in most cases.

The aim of this paper is to give a short review of the capabilities of the universal Nesvetay computer code [10] (Nesvetay is a river in Rostov region in Russia) as applied to the numerical simulation of the flow of high-speed monatomic gas around objects of irregular shape for large flight altitudes. This code has been developed by the author of this paper during a number of recent years (see [11–15]). It implements Godunov-like schemes adapted for solving the three-dimensional kinetic equations with the approximate (model) collision operator proposed by Shakhov [8] (S-model).

The main features of the Nesvetay code are the ability to use both multi-block structured and completely unstructured meshes in the physical and phase spaces, fast implicit discretization method with respect to time for solving steady problems, and the support of the single and multilevel OpenMP + MPI parallel computing model, which makes it possible to perform computations on systems with dozens of thousands of thousands of x86 cores.

1. GOVERNING EQUATIONS

We consider the exterior flow of monatomic rarefied gas around a three-dimensional body. The unperturbed flow is characterized by the number density n_∞, pressure p_∞, temperature T_∞, velocity u_∞, and viscosity μ_∞. The state of the monatomic gas is described by the velocity distribution function $f = f(t, \mathbf{x}, \boldsymbol{\xi})$, where (ξ_1, ξ_2, ξ_3) are the components of the molecular velocity vector in the directions (x_1, x_2, x_3), respec-

tively, and t is the physical time. The Boltzmann kinetic equation for $f(t,\mathbf{x},\xi)$ with the S-model collision operator [8] has the form

$$\frac{\partial f}{\partial t}+\xi_\alpha\frac{\partial f}{\partial x_\alpha}=J,\quad J=\nu(f^+-f),\quad \nu=\frac{p}{\mu},$$
$$f_M=\frac{n}{(2\pi R_gT)^{3/2}}e^{-c^2},\quad f^+=f_M\left[1+\frac{4}{5}(1-\mathrm{Pr})S_\alpha c_\alpha\left(c^2-\frac{5}{2}\right)\right], \tag{1}$$
$$S_i=\frac{1}{n}\int c_ic^2 fd\xi,\quad \mathbf{c}=\frac{\xi-\mathbf{u}}{\sqrt{2R_gT}}.$$

Here, Pr is the Prandtl number (Pr = 1 corresponds to the BGK model [7]), and R_g is the gas constant. The summation is made over repeating Greek indexes. We also assume the power dependence of viscosity on temperature with exponent ω:

$$\mu(T)=\mu_\infty\left(\frac{T}{T_\infty}\right)^\omega. \tag{2}$$

The macrosopic parameters, such as the number n and mass ρ densities, mean velocity vector $\mathbf{u}=(u_1,u_2,u_3)$, pressure p, temperature T, and heat flux $\mathbf{q}=(q_1,q_2,q_3)$ are expressed as integrals of the velocity distribution function (m is the molecule mass):

$$n=\int fd\xi,\quad n\mathbf{u}=\int\xi fd\xi,\quad \frac{3}{2}mnR_gT+\frac{1}{2}mnu^2=\frac{1}{2}m\int\xi^2fd\xi,$$
$$\mathbf{q}=\frac{1}{2}m\int\mathbf{v}v^2fd\xi,\quad \mathbf{v}=\xi-\mathbf{u},\quad \rho=mn,\quad p=\rho R_gT. \tag{3}$$

The boundary conditions are formulated as follows. On the body surface, we set the condition of diffusive scattering of molecules with complete thermal accommodation to the surface temperature T_w:

$$f=f_w=\frac{n_w}{(2\pi R_gT_w)^{3/2}}\exp\left(-\frac{\xi^2}{2R_gT_w}\right). \tag{4}$$

For simplicity, we assume in this paper that the surface temperature is constant and determined by the problem conditions. The density of reflected particles n_w is determined from the impermeability condition. At the infinity upstream, the unperturbed flow condition is specified:

$$f=f_\infty(\xi)=\frac{n_\infty}{(2\pi R_gT_\infty)^{3/2}}\exp\left(-\frac{(\xi-\mathbf{u}_\infty)^2}{2R_gT_\infty}\right).$$

We also assume that the distribution function downstream is close to the locally Maxwell function with the parameters determined by the problem solution.

The initial value of the distribution function $f(0,\mathbf{x},\xi)$ is assumed to be equal to the locally Maxwell function with the given field of the gas density, velocity, and temperature distribution field.

2. THE NUMERICAL SOLUTION METHOD

In this work, we use the discrete ordinate method with grids of arbitrary types both in the physical and velocity spaces. This feature of the method distinguishes it from the majority of other methods of solving the kinetic equation described in the literature, and it makes the proposed method highly flexible and efficient for calculating exterior flows around bodies of irregular shapes. We introduce in the velocity space a bounded computation domain with the grid nodes $\xi_j=(\xi_{1j},\xi_{2j},\xi_{3j})$. The total number of grid nodes is denoted by N_ξ. The functions $\mathbf{f}$ and $\mathbf{f}^{(S)}$ are defined at the centers of the velocity grid, and we interpret them as vectors of length N_ξ with the components

$$f_j=f(t,\mathbf{x},\xi_j),\quad f_j^{(S)}=f^{(S)}(t,\mathbf{x},\xi_j).$$

The kinetic equation (1) can be written as a system of N_ξ equations, and in vector form it is

$$\frac{\partial}{\partial t}\mathbf{f} + \frac{\partial}{\partial x_\alpha}(\mathbf{\Xi}_\alpha \circ \mathbf{f}) = \mathbf{J}, \quad \mathbf{J} = \nu(\mathbf{f}^{(S)} - \mathbf{f}). \tag{5}$$

Here, $\mathbf{\Xi}_k$ is the vector the components of which are the kth components of the molecular velocity at all grid nodes: $\mathbf{\Xi}_k = (\xi_{k1}, \xi_{k2}, \xi_{k3}, \ldots \xi_{kN_\xi})^{\mathrm{T}}$; by $\circ$ we denote the operation of componentwise multiplication of two vectors: $c = a \circ b$ is the vector with the components $c_i = a_i b_i$.

System (5) is written in conservative form. The number of equations is determined by the grid size in the velocity space, and it can be large (tens or even hundreds of thousands of equations). To solve system (5), we use a special version of the upwind TVD scheme of the Godunov type.

In the physical space, the computation mesh is decomposed into control volumes (cells) V_i of tetrahedral, pyramidal, hexahedral, or prismatic shape. Each cell is formed by a number of triangular or rectangular faces A_{li}, where l is the face index. The total number of cells is N_{space}. The integration of system (5) over the cell V_i and the standard approximation of integrals of the fluxes and of the right-hand side yields the semi-discrete scheme for the values of the distribution function $\mathbf{f}_i$

$$\frac{\partial \mathbf{f}_i}{\partial t} = \mathbf{R}_i = -\frac{1}{|V_i|}\sum_{l=1} \mathbf{\Phi}_{li} + \mathbf{J}_i, \quad \mathbf{\Phi}_{li} = \int_{A_{li}} (\xi_{li} \circ \mathbf{f}) dS, \tag{6}$$

where the components of the vector ξ_{li} are equal to the values of the projection of the molecular velocity on the external unit normal to the face l of the spatial cell V_i.

The procedure for finding the flux $\mathbf{\Phi}_{li}$ for the face l of cell V_i on an arbitrary unstructured grid is thoroughly described in [11, 12, 14, 15] and consists of two stages. At the first stage, the solution on the mesh faces is reconstructed given the known mean values in the cells (see [16–18]) to achieve the second approximation order with respect to space. In the general case, the values $\mathbf{f}_{li}$ of the distribution function on the interior side of the face l of V_i are computed by the mean values in the cell V_i and its neighbors by the formula

$$\mathbf{f}_{li} = \mathbf{f}_i + \mathbf{f}_{li}^{\text{cor}}.$$

The correction $\mathbf{f}_{li}^{\text{cor}}$ can be computed using two approaches. In the most general method, the correction is expressed using the least squares method written in the local system of coordinates [19, 20] in terms of the mean values V_{m_i} in the stencil cells by the formula

$$\mathbf{f}_{li}^{\text{cor}} = \psi_i^{3d}\left(\sum_{m=0}^{M} g_{iml}\mathbf{f}_{m_i} - \mathbf{f}_i\right). \tag{7}$$

The coefficients g_{iml} are determined only by the mesh geometry, and they are found at the stage of the computation initialization. Below, we denote this method by TVD3D. An example of the reconstruction stencil for the least squares method is shown in Fig. 1. For hexahedral meshes, the locally one-dimensional approach can be used, in which the correction values are found by interpolation along the mesh lines in the direction of the face normal:

$$\mathbf{f}_{li}^{\text{cor}} = \psi_{li}^{1d}(\mathbf{S}_L, \mathbf{S}_R)\Delta_l, \tag{8}$$

where Δ_l is the distance from the center of cell i to the center of face l, and $\mathbf{S}_L$ and $\mathbf{S}_R$ are the left and the right estimates of the solution slope. This method is denoted by TVD1D. For both types of reconstruction, the function ψ is the so-called slope limiter, which is typically used to suppress the slopes of type minmod [16, 21].

An important part of the numerical method is the algorithm approximating the boundary conditions. To compute the boundary condition of the mirror reflection from the symmetry plane, the velocity grid is constructed so as to ensure that the velocity vector of the reflected molecule $\xi_1 = \xi - 2\xi_n\mathbf{n}$ hits a node of the velocity grid. In this case, the computation of the boundary condition is trivial: $f(t, \mathbf{x}, \xi) = f(t, \mathbf{x}, \xi_1)$. For all faces of the mesh cells lying on the body surface, integration with respect to ξ at the given surface temperature T_w gives density of the reflected molecules n_w so as to exactly satisfy the impermeability condition.

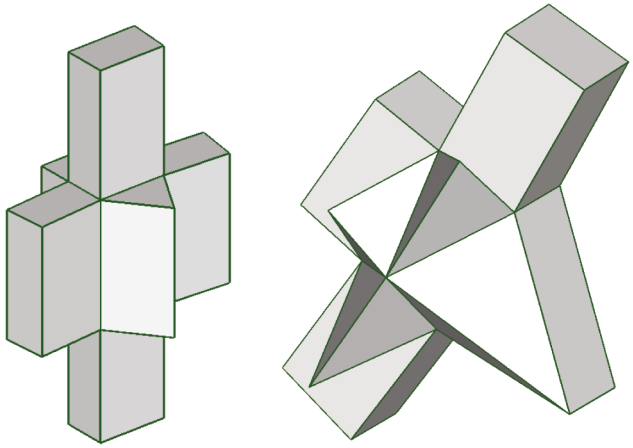

Fig. 1. Examples of reconstruction stencils for the TVD3D method (7) on an unstructured spatial mesh with arbitrarily shaped cells.

At the second stage, the resulting values $\mathbf{f}^-$ and $\mathbf{f}^+$ of the distribution function on both sides of each mesh face are used to find the final value Φ_{li} by solving the Riemann problem for the linear equation in the direction perpendicular to the face:

$$\mathbf{\Phi}_{li} = \frac{1}{2}\xi_{li} \circ \left[\mathbf{f}^- + \mathbf{f}^+ - \mathrm{sign}(\xi_{li}) \circ (\mathbf{f}^+ - \mathbf{f}^-)\right]|A_{li}|, \tag{9}$$

where $|A_{li}|$ is the face area. In addition to the exact formula (9), the approximate solution based on Rusanov's approach [22], in which the maximum absolute value of the molecular velocity is used as the velocity bound, may be used. For the mesh faces lying on the boundaries of the computation domain in the physical space, $\mathbf{f}^+$ is found from the boundary condition.

The computation of the model (approximate) collision integral $\mathbf{J}$ (the grid indexes in space and time step are omitted for brevity) requires macroscopic parameters to be known. Let b_j be the weights of the second-order quadrature rule. The straightforward approximation of expressions (3) for the gas macroparameters is

$$(\mathbf{U}, \mathbf{q}) = \left(n, n\mathbf{u}, \frac{3}{2}nT + n\mathbf{u}^2, \mathbf{q}\right) = \sum_{j=1}^{N_\xi} \left(1, \xi, \xi^2, \frac{1}{2}\mathbf{v}v^2\right)_j f_j b_j. \tag{10}$$

The numerical integration of the semi-discrete scheme (6) with the weights 1, ξ, and ξ^2 yields a discrete analog of the equations of mass, momentum, and energy conservation

$$\frac{\partial}{\partial t}\mathbf{U} + D_h(\mathbf{\Pi}) = \epsilon_{\mathrm{Kn}}, \quad \epsilon_{\mathrm{Kn}} = \sum_{j=1}^{N_\xi} (1, \xi, \xi^2)_j^{\mathrm{T}} J_j b_j. \tag{11}$$

Here, $\mathbf{\Pi}$ is the tensor of physical fluxes. If the integration with respect to ξ is exact, then the numerical method is conservative, so that $\epsilon_{\mathrm{Kn}} \equiv \mathbf{0}$. However, if (10) is substituted into Eqs. (11), a nonconservative scheme is obtained (see [23]), and the error is inversely proportional to the Knudsen number $|\epsilon_{\mathrm{Kn}}| \approx \frac{1}{\mathrm{Kn}} O(\Delta\xi^2)$. To perform computations with a large number of steps or small Knudsen numbers, the condition $|\epsilon_{\mathrm{Kn}}| = 0$ should be satisfied.

The main idea underlying the computation of macroscopic parameters [23] is to directly approximate the conditions imposed on the model collision integral that were used in [8] in the derivation of the S-model. The vector of primitive variables $\mathbf{W} = (n, \mathbf{u}, T, \mathbf{q})^{\mathrm{T}}$ is found from the system of equations

$$\mathbf{H}(\mathbf{W}) = \sum_{j=1}^{N_\xi} \begin{pmatrix} 1 \\ \xi \\ \xi^2 \\ \mathbf{v}v^2 \end{pmatrix}_j (f^{(S)} - f)_j b_j + \begin{pmatrix} 0 \\ \mathbf{0} \\ 0 \\ 2\,\mathrm{Pr}\,\mathbf{q} \end{pmatrix} = 0. \tag{12}$$

For each spatial cell i, the system of eight equations (12) is solved using the Newton method

$$M(\mathbf{W}^{s-1})(\mathbf{W}^s - \mathbf{W}^{s-1}) = -\mathbf{H}(\mathbf{W}^{s-1}), \quad M = \frac{\partial \mathbf{H}}{\partial \mathbf{W}}, \quad s = 1, 2, \ldots . \tag{13}$$

As the initial approximation, we use the values obtained by formulas (10). In the special case $\mathrm{Pr} = 1$, the last three equations can be dropped, and system (12) is reduced to the procedure proposed in [24, 25].

The computation of the Jacobian matrix M in system (12), which consists of discrete sums of the derivatives $f^{(S)}$ over to the macroscopic variables, is the slow part of the Newton method. The exact computation of M is computationally costly, especially for complex kinetic models, such as Rykov's model of diatomic gas [9]. If we replace the numerical integration in the expression for M by the exact (analytical) integration, then we can obtain an approximate analytical representation of M in terms of the gas macroparameters [11, 26]. The use of the approximate formula for M considerably reduces the computation time even though the quadratic convergence of iterations is lost.

In this paper, we use the implicit one-step scheme without iterations on the upper time level for discretization with respect to time; this scheme is derived from (6) in the conventional way:

$$\frac{\Delta \mathbf{f}_i}{\Delta t} = \mathbf{R}_i^{n+1} = \mathbf{R}_i^n + \left(\frac{\partial \mathbf{R}}{\partial \mathbf{f}}\right)_i^n \Delta \mathbf{f}_i, \quad \Delta \mathbf{f}_i = \mathbf{f}_i^{n+1} - \mathbf{f}_i^n. \tag{14}$$

To compute the increment of the distribution function in time, we make the approximate linearization (14)

$$\mathbf{\Phi}_{li}^{n+1} \approx \mathbf{\Phi}_{li}^n + \frac{\partial \mathbf{\Phi}_{li}^n}{\partial \mathbf{f}_i^n} \circ \Delta \mathbf{f}_i + \frac{\partial \mathbf{\Phi}_{li}^n}{\partial \mathbf{f}_{i_l}^n} \circ \Delta \mathbf{f}_{i_l}, \quad \mathbf{J}_i^{n+1} \approx \mathbf{J}_i^n - \nu_i^n \Delta \mathbf{f}_i.$$

Here, $\mathbf{f}_{i_l}$ is the value of the distribution function in the cell with the index i_l that is adjacent to the cell V_i through the face l. In the further simplifications, we assume the numerical flux on the left-hand side is approximated by the first-order upwind scheme using the exact Riemann problem solution or Rusanov's approach. By rearranging terms and explicitly writing out the coefficient of $\Delta \mathbf{f}_i$, we obtain

$$\mathbf{d}_i \circ \Delta \mathbf{f}_i + \Delta t \sum_l \mathbf{c}_{li} \circ \Delta \mathbf{f}_{i_l} = \Delta t \mathbf{R}_i^n. \tag{15}$$

The quantity $\mathbf{R}_i^n$ is found accurate to the second order given the known values on the lower time level t^n. To solve (15), we use an approximate factorization of the sparse matrix on the basis of the approach proposed in [27, 28] for fluid dynamics equations. Then, the values $\Delta \mathbf{f}_i$ are found using the conventional backward and forward elimination of the LU method.

To solve the problems of high-speed rarefied gas flows around bodies with complicated shapes more efficiently and reliably, two improvements to the basic numerical method were made. The first improvement is the method of constructing the nonuniform adaptive grid in the velocity space [14, 15]. Near $\xi = U_\infty$ (the incident flow) and $\xi = 0$ (the body surface), cubic subdomains are defined in which the cubic grid with $\Delta\xi = 0.5\sqrt{2R_gT_\infty}$ and $\Delta\xi = 0.5\sqrt{2R_gT_w}$, respectively, are used. In the other part of the domain, pyramids and tetrahedra the size of which smoothly grows to $\approx 0.5\sqrt{2R_gT_{sw}}$, where T_{sw} is the temperature estimate after the shock front, are used. Typically, the grid is constructed in a quarter of the space taking into account the problem symmetry planes; then, the Nesvetay preprocessor extends the grid to the other parts of the domain in the velocity space. This method of constructing the velocity grid requires certain knowledge about the problem to be solved; however, it is much simpler than the adaptive octree used in [4, 5].

The second improvement uses the nonuniform discretization in the physical space. As a rule, structured grids which are clustered to the surface are preferable for computing high-speed external flows. However, for irregularly shaped bodies, such grids can contain a small number of poor quality cells, e.g., strongly skewed cells. Experience shows that the most reliable second-order scheme is the TVD3D approach based on the least squares method; however, it can result in the loss of formal convergence to the steady solution. The TVD1D method provides improved accuracy in the most loaded parts of the surface and ensures the formal convergence to the steady solution. However, it can give nonphysical values of macroscopic parameters in the poor grid cells.

In this paper, it is proposed to use the adaptive switching between the methods TVD1D and TVD3D. The method TVD1D is the basic one. As the solution approaches the steady state, the Nesvetay code creates a list of poor cells in which the temperature is below a certain small value and switches the reconstruction procedure in these cells to the TVD3D method. The resulting numerical method converges in the integral norm while avoiding nonphysical temperature values.

On the whole, the solution procedure consists of the following steps. First, the flow field is initialized with the values of the incident flow macroparameters or by solving the Navier–Stokes equations of viscous gas using a third-party code (e.g., [29, 30]). Next, the preliminary kinetic solution is obtained using the first-order method and the BGK model. The final solution is obtained by using the distribution function obtained above as the initial condition for the second-order scheme and the S-model. This algorithm is able to construct solutions for arbitrarily large Mach numbers of the incident flow.

3. SOFTWARE PACKAGE NESVETAY

The software package Nesvetay [13] includes a computation kernel, kinetic solver, and mesh preprocessors. The computation kernel contains a set of classes and modules implementing the basic operations needed for performing computations: procedures for reading spatial grids in various formats and construction of mesh connectivity, algorithms for reconstructing scalar functions by the least squares method on an arbitrary grid, and input–output procedures of spatial and surface data in the Tecplot format. The kinetic solver is an add-in over the kernel that implements the numerical scheme for solving the kinetic equation. The grid preprocessors are used for decomposing the computation grid for parallel computations. The total size of the code is about 20000 lines in Fortran 2003/2008 with elements of object-oriented programming. Microsoft Visual Studio and the Intel Fortran compiler included in Intel Parallel Studio were used as the development environment.

A key feature of the proposed software package is the use of the two-level parallel computation model OpenMP + MPI, which has been recently intensively developed as applied to gas-dynamics computations, e.g., see [31, 32].

In Nesvetay, each level of parallel implementation is based on a decomposition of the computation grid. At the upper level, the MPI technology of data exchange between the supercomputer nodes is used. For distributing computations over the supercomputer nodes, the grid decomposition in the velocity space or in the physical space, which is conventional for the computational fluid dynamics, may be used. At the low level of the organization of parallel computations, the grid decomposition into blocks in the physical space and the OpenMP technology is always used. For the majority of solution method procedures, it is sufficient to use simple OMP loops with dynamic balancing. However, the parallel multithreaded implementation of the LU-SGS method for solving the system of equations for the increment of the distribution function requires a special adaptation of the solution method to ensure that the convergence rate to the steady solution does not deteriorate.

Thus, the OpenMP + MPI implementation of the proposed approach makes it possible to use an arbitrary combination of MPI processes and OpenMP threads in the supercomputer node. Below, we mainly use the version of MPI decomposition in the velocity space because it is most convenient from the practical point of view. Note that the decomposition of the velocity grid for performing MPI computations for solving the exact Boltzmann equation using an explicit difference scheme was probably first used in [33].

The results of testing the scalability of the parallel version of the Nesvetay code on various Russian supercomputers can be found in [12, 14, 34]. The best results in terms of the number of used processors were achieved on the RSC PetaStream system [35] installed in the supercomputer center "*Polytechnic*" of the Peter the Great St. Petersburg Polytechnic University. Each node of this cluster includes one coprocessor Intel Xeon Phi 5120D (60 physical cores, 240 hyperthreads, clock rate 1.053 GHz, RAM 8 GB). Up to 256 nodes (61440 hyperthreads) were used in the computations, and the efficiency of about 75% was achieved, which is at the best level of computational fluid dynamics [31, 32].

4. COMPUTATION EXAMPLES

In the analysis of results, the gas rarefaction degree is characterized by the rarefaction factor δ, which is inversely proportional to the Knudsen number Kn determined on the basis of the free path λ_∞ in the incident gas flow and the given length scale l_∞:

$$\delta = \frac{l_\infty p_\infty}{\mu_\infty v_\infty} = \frac{8}{5\sqrt{\pi}}\frac{1}{\mathrm{Kn}}, \quad \mathrm{Kn} = \frac{\lambda_\infty}{l_\infty}, \quad v_\infty = \sqrt{2R_g T_\infty}.$$

The first benchmark problem is the planar argon flow around a planar circular cylinder of radius 6 inches ($r_{cyl} = 0.1524$ m) [15, 34]. The problem was solved for the incident flow velocity $U_8 = 6585$ m/s, the flow temperature $T_\infty = 200$ K, and the surface temperature $T_w = 1500$ K. Two values of the incident flow density $\rho_\infty = 1.127\times10^{-6}$ kg/m^3 and 2.818×10^{-5} kg/m^3, which at $l_\infty = r_{cyl}$ correspond to the rarefaction parameter $\delta = 1.6$ and 40, respectively, were used. The corresponding Knudsen numbers are Kn = 0.56 and 0.0225. In all cases, the exponent in the viscosity law was $\omega = 0.734$. The Prandtl number was Pr = 2/3. The mesh in the physical space consisted of 115×40 cells in the plane $x - y$ and three cells on the axis z. The height of the first cell in the near-wall layer was $h_n = 10^{-4} r_{cyl}$. The nonuniform velocity grid with refinement to $\xi = 0$ and $\xi = U_\infty$ consisted of 35 720 nodes. The solution of the problem took 1000–3000 core-hours, depending on the value of δ.

Figure 2 illustrates the comparison of the distribution of the pressure and heat transfer coefficients on the cylinder surface obtained by solving the model kinetic Shakhov and BGK equations with the results of paper [36] obtained by the MONACO code [37] based on the direct simulation Monte Carlo (DSMC) method. The results obtained by the DSMC and by solving the Shakhov model equation are in excellent agreement for all δ; the maximum difference at the stagnation point does not exceed 2%. The use of the BGK model gives a noticeable error in the heat transfer coefficient for $\delta = 40$. Figure 3 illustrates the comparison of the temperature profiles on the stagnation line in the flow field. On the whole, the computation results obtained by the S-model and the DSMC method are close, except for the tail of the shock wave. The use of the BGK model gives a considerable error in the "step" of the temperature profile beyond the shock front at $\delta = 40$.

In [38], the computation results obtained using the S-model were compared with the results obtained by solving the exact Boltzmann equation with the viscosity law corresponding to the rigid sphere model. Good agreement between these results for the distribution of the surface coefficients for $M_\infty = 10$ was obtained. The computations were performed using the Nesvetay and the UFS [2, 4] codes; also see [39, 40].

Thus, in these computations, the good accuracy of the S-model kinetic equation in problems of the high-speed flow around blunt bodies, including the computation of heat transfer on the surface, was demonstrated for the first time.

As the second benchmark problem, we consider the air flow around the three-dimensional model of an aerospace vehicle of the Central Aerodynamic Institute (TsAGI) at large altitudes without taking into account the internal degrees of freedom. The model has an complicated shape—it consists of a fuselage with a blunted nose, two wings, a vertical fin, and a flap. The total length of the body with the flap is 10 meters. Due to its geometric complexity, the need to use a spatial grid with a large number of poor cells and the velocity grid for the flow incident at the angle of attack, the construction of solution to this problem is an excellent test. For applied (engineering) computations, it is critically important to obtain a solution in a short time.

The principal ability to construct a numerical solution to this problem using the Nesvetay code for the incident flow with Mach numbers $M_\infty \geq 10$ and various angles of attack was demonstrated in [14, 15, 34]. This is possible due to the use of a combination of the adaptive velocity grid and an efficient implicit method. In this work, the computation time is significantly reduced due to the use of a nonuniform approximation of the transport operator on the spatial grid in the Nesvetay code.

To estimate the actual computation errors, the results are compared with the results obtained using the code [41–46], which implements a modern scheme of direct simulation Monte Carlo method. In the computations using the SMILE code, the flow parameters corresponded to air (the specific heat ratio $\gamma = 1.4$ and $R_g = 287.6$ J/(kg K)) with the "frozen" internal degrees of freedom for the given altitude H, the Mach number M_∞, and the angle of attack α. The physical model used in these computations is strictly speaking not equivalent to the S-model; for this reason, the comparison is evaluative. The computations using the SMILE code were performed by E. A. Bondar', P. V. Vashchenkov, and A. A. Shevyrin (Khristianovich Institute of Theoretical and Applied Mechanics, Siberian branch of the Russian Academy of Sciences).

In [34, 47], acceptable agreement between the Nesvetay and SMILE computations with the "frozen" internal degrees of freedom for the problem parameters $H = 90$ km, $M_\infty = 10$, and $\alpha = 25$ was obtained. In this paper, we construct the solution for the more realistic conditions of $H = 100$ km and $M_\infty = 25$. The corresponding incident flow parameters for air are $\rho_\infty = 5.550\times10^{-7}$ kg/m^3, $p_\infty = 0.0319$ Pa,

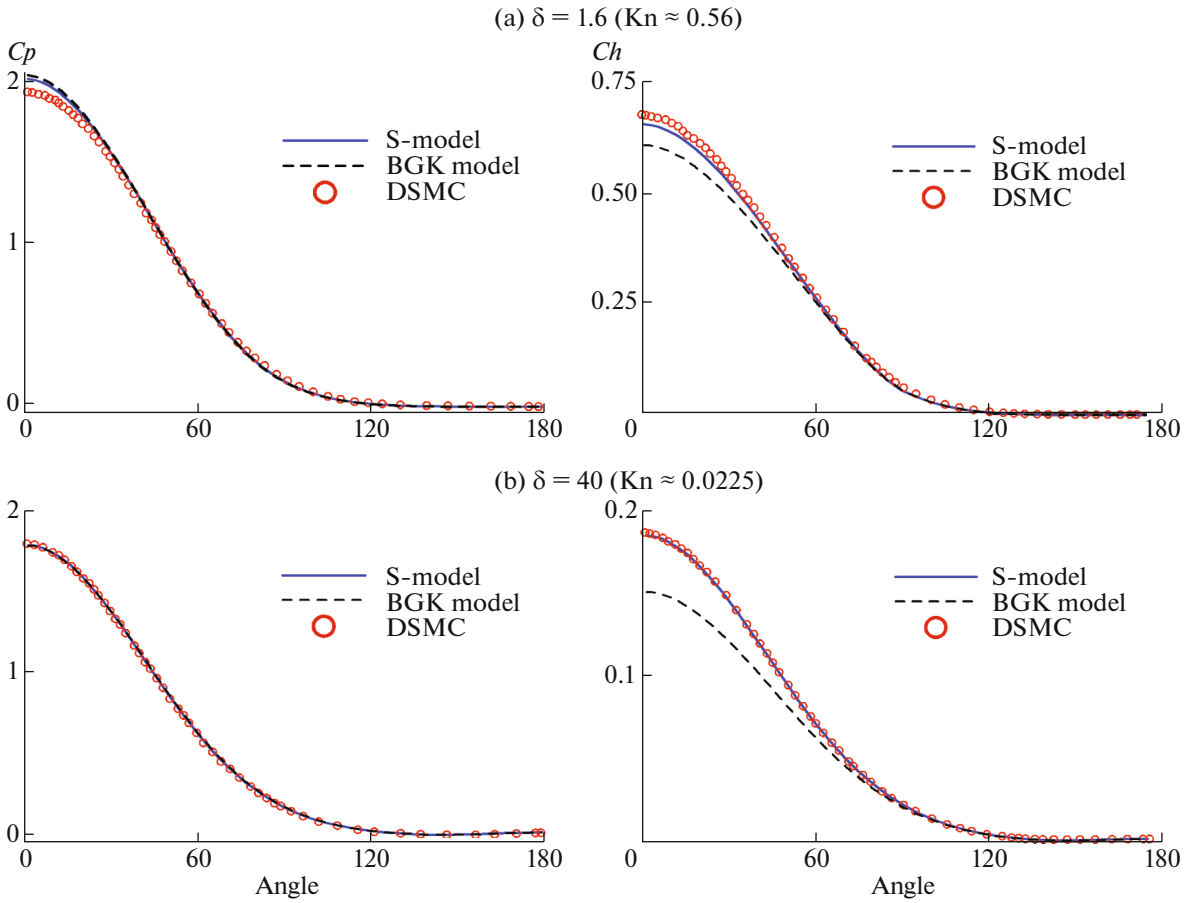

Fig. 2. Distribution of the pressure c_p, friction c_f, and heat transfer c_h coefficients over the cylinder surface in the argon flow for $M_\infty = 25$. The solid line corresponds to the S-model, the dashed line to the BGK model, and dots to the direct simulation Monte Carlo (DSMC) method [36].

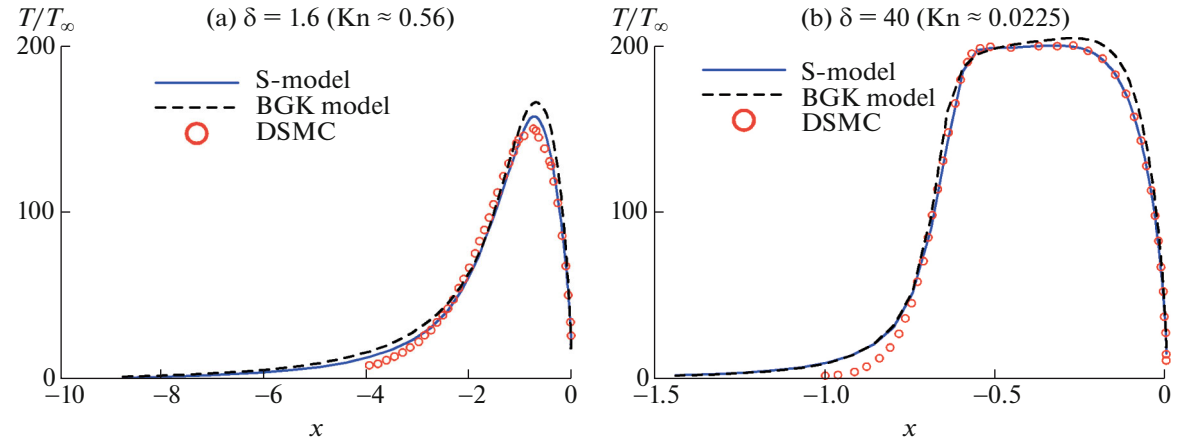

Fig. 3. Comparison of the dimensionless temperature profiles along the stagnation line T/T_∞ in the argon flow around a cylinder for $M_\infty = 25$. The notation is the same as in Fig. 2.

$U_\infty = 7092$ m/s, $T_\infty = 199.34$ K, and the surface temperature $T_w = 300$ K (in [34, 47], $T_w = 1500$ K). The Prandtl number in Eq. (1) was Pr = 0.71. The rarefaction parameter was δ = 5.43 on the basis of the characteristic size $l_\infty = 1$ m. The algorithm for the collision computation used in SMILE approximately cor-

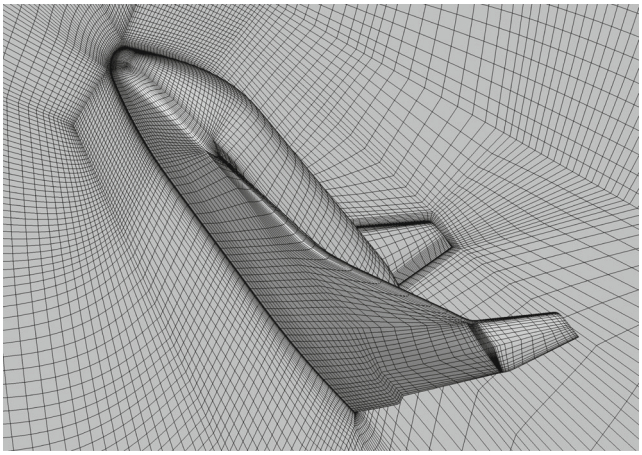

Fig. 4. Computation mesh in the physical space for the flow around an aerospacevechile.

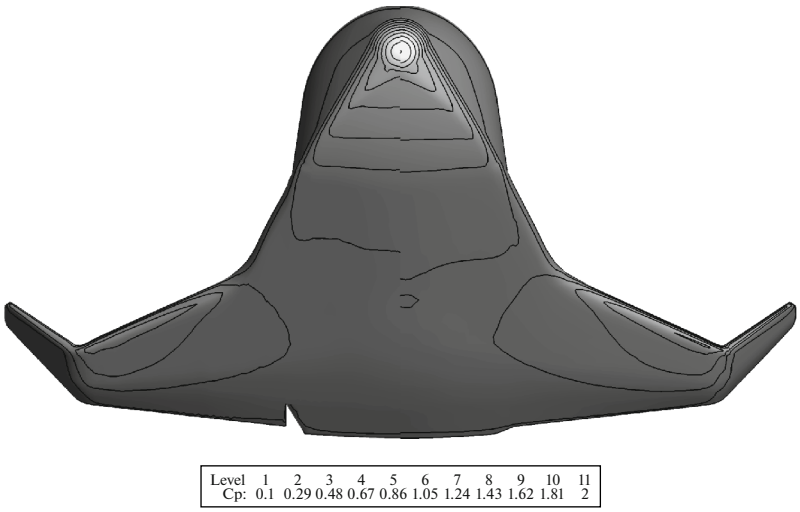

Fig. 5. Comparison of the pressure coefficient distribution c_p for $H = 100$ km, $\alpha = 25$, and $M_\infty = 25$. SMILE on the left and Nesvetay on the right.

responds to the viscosity law (2) with the parameters $\mu_\infty = 1.74 \times 10^{-5}$ and $\omega = 0.734$; these constants in the viscosity law were also used in the computations by the Nesvetay code.

A detailed description of the parameters of the computation meshes in the physical space can be found in [47]. The SMILE code uses a multidimensional Cartesian computation mesh adapted for the domains in which the flow is strongly nonequilibrium, such as shock fronts and near-wall domains. The Nesvetay code uses the grid model in the physical space based on a multiblock grid consisting of 159 blocks with the total number of 568 thousand cells (see Fig. 4). The height of the first cell adjacent to the body surface was 10^{-3} m. The grid in the velocity space was constructed as in the case of flow around the cylinder—it contained 32144 nodes, so that the total number of degrees of freedom (cells in the 6-dimensional grid) was 18 billion. The solution of the problem using the Nesvetay code took 5000 core-hours of computer time.

Figures 5 and 6 illustrate the comparison of the computation results for c_p and c_h. The pressure coefficient values are in good agreement, while the value of the thermal transfer coefficient c_h obtained by SMILE ($c_h = 0.77$) at the model nose, which is most difficult to compute, is slightly greater than the value produced by Nesvetay ($c_h = 0.65$). The difference of 16% can be explained by the use of the significantly different equations, grids, and numerical methods. On the whole, good agreement of the computations

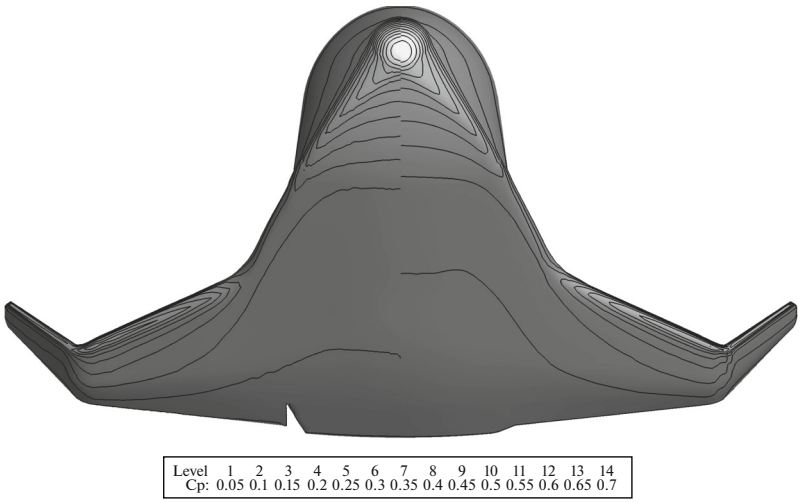

Fig. 6. Comparison of the thermal transfer coefficient distribution c_h for $H = 100$ km, $\alpha = 25$, and $M_\infty = 25$. SMILE on the left and Nesvetay on the right.

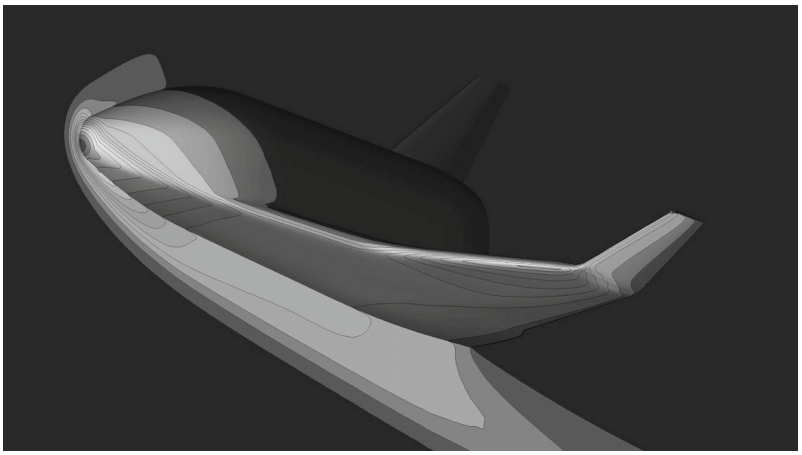

Fig. 7. Contour lines of the dimensionless pressure p/p_∞ obtained by the Nesvetay code for $H = 100$ km, $\alpha = 25$, and $M_\infty = 25$.

based on the S-model and by the DSMC method in the computation of the flow around an irregularly shaped 3D body and a large incident flow velocity was obtained.

Figure 7 shows the contour lines of the dimensionless pressure obtained using the Nesvetay code. On the whole, we have a typical pattern of high-speed rarefied gas flow around a body; it includes the forming bow shock wave and the bottom region with reverse flow. The ratio of the pressure in the stagnation region near the body nose to the pressure in the bottom region is greater than 20000. Nonetheless, the Nesvetay code is able to construct the solution to the problem.

CONCLUSIONS

The capabilities of the Nesvetay package of parallel programs, which has been developed by the author during several years in the department of mechanics of the Federal Research Center "Computer Science and Control" of the Russian Academy of Sciences, for simulating external high-speed rarefied gas flow around various bodies are described. The results demonstrate good accuracy and reliability of the package as applied to the computations of flows around bodies of complicated shapes up to the Mach numbers $M_\infty = 25$ using modern Russian supercomputers.

FUNDING

This work was supported by the Russian Foundation for Basic Research, project nos. 18-08-00501 and 18-07-01500.

ACKNOWLEDGMENTS

I am grateful to my colleagues E.M. Shakhov and A.A. Frolova for useful discussions and to Ye.A. Bondar, P.V. Vashchenkov, and A.A. Shevyrin (Khristianovich Institute of Theoretical and Applied Mechanics, Siberian branch of the Russian Academy of Sciences) for the computation results obtained using the package SMILE. The work was performed using the resources of the supercomputer center of the Lomonosov Moscow State University [48], the Joint Supercomputer Center (JSCC) of the Russian Academy of Sciences, the supercomputer center "*Polytechnic*" of the Peter the Great St. Petersburg Polytechnic University, and Moscow Institute of Physics and Technology.

REFERENCES

1. S. K. Godunov, "A difference method for the numerical calculation of discontinuous solutions to fluid dynamics equations," Mat. Sb. **47** (89), 271–306 (1957).
2. V. I. Kolobov, R. R. Arslanbekov, V. V. Aristov, A. A. Frolova, and S. A. Zabelok, "Unified solver for rarefied and continuum flows with adaptive mesh and algorithm refinement," J. Comput. Phys. **223**, 589–608 (2007).
3. Yu. A. Anikin, Yu. Yu. Kloss, D. V. Martynov, and F. G. Cheremisin, "Computer simulation and analysis of the Knudsen experiment of 1910," Nano Mikrosist. Tekhn., No. 8, 6–14 (2010).
4. R. R. Arslanbekov, V. I. Kolobov, and A. A. Frolova, "Kinetic solvers with adaptive mesh in phase space," Phys. Rev. E **88**, 063301 (2013).
5. C. Baranger, J. Claudel, N. Herouard, and L. Mieussens, "Locally refined discrete velocity grids for stationary rarefied flow simulations," J. Comput. Phys. **257**, 572–593 (2014).
6. G. Dimarco, R. Loubere, and J. Narski, "Towards an ultra efficient kinetic scheme. Part III: High-performance computing," J. Comput. Phys. **284**, 22–39 (2015).
7. P. L. Bhatnagar, E. P. Gross, and M. Krook, "A model for collision processes in gases. I. Small amplitude processes in charged and neutral one-component systems," Phys. Rev. **94**, 511–525 (1954).
8. E. M. Shakhov, "On a generalization of the relaxation kinetic Krook equation, Izv. Akad. Nauk SSSR, Ser. Mekh. Zhidkosti Gaza, No. **5**, 142–145 (1968).
9. V. A. Rykov, "Model kinetic equation for the gas with rotational degrees of freedom,", Izv. Akad. Nauk SSSR, Ser. Mekh. Zhidkosti Gaza, No. 6, 107–115 (1975).
10. V. A. Titarev, "Software package Nesvetay-3D for simulating three-dimensional flows of monoatomic rarefied gas," Certificate of State Registration of computer programs 20176616295, 2017.
11. V. A. Titarev, "Implicit numerical method for computing three-dimensional rarefied gas flows on unstructured meshes," Comput. Math. Math. Phys. **50**, 1719–1733 (2010).
12. V. A. Titarev, M. Dumbser, and S. V. Utyuzhnikov, "Construction and comparison of parallel implicit kinetic solvers in three spatial dimensions," J. Comput. Phys. **256**, 17–33 (2014).
13. V. A. Titarev, "Software package Nesvetay-3D for simulating 3D flows of rarefied monatomic gas," Nauka Obraz., No. 6, 124–154 (2014).
14. V. A. Titarev, "Numerical modeling of high-speed rarefied gas flows over blunt bodies using model kinetic equations," Europ. J. Mech. B Fluids, Special Issue on Non-equilibrium Gas Flows **64**, 112–117 (2017).
15. V. A. Titarev, "Application of model kinetic equations to hypersonic rarefied gas flows," Comput. Fluids, Special issue "Nonlinear flow and transport," **169**, 62–70 (2018).
16. V. P. Kolgan, "Application of the minimum derivative principle for constructing finite difference schemes for the calculation of discontinuous solutions in fluid dynamics," Uchen. Zapiski TsAGI **3** (6), 68–77 (1972).
17. V. P. Kolgan, "Application of the principle of minimizing the derivative to the construction of finite-difference schemes for computing discontinuous solutions of gas dynamics," J. Comput. Phys. **230**, 2384–2390 (2011).
18. B. Van Leer, "Towards the ultimate conservative difference scheme V: A second-order sequel to Godunov's method," J. Comput. Phys. **32**, 101–136 (1979).
19. M. Dumbser and M. Käser, "Arbitrary high order non-oscillatory finite volume schemes on unstructured meshes for linear hyperbolic systems," J. Comput. Phys. **221**, 693–723 (2007).
20. M. Dumbser, M. Käser, V. A. Titarev, and E. F. Toro, "Quadrature-free non-oscillatory finite volume schemes on unstructured meshes for nonlinear hyperbolic systems," J. Comput. Phys. **226**, 204–243 (2007).
21. T. J. Barth and P. O. Frederickson, "Higher order solution of the Euler equations on unstructured grids using quadratic reconstruction," AIAA paper no. 90-0013, *28th Aerospace Sciences Meeting*, 1990.
22. V. V. Rusanov, "Computation of nonstationary shock waves with obstacles," Zh. Vychisl. Mat. Mat. Fiz. **1** (2), 267–279 (1961).
23. V. A. Titarev, "Conservative numerical methods for model kinetic equations," Comput. Fluids **36**, 1446–1459 (2007).

24. L. Mieussens, "Discrete-velocity models and numerical schemes for the Boltzmann-BGK equation in plane and axisymmetric geometries," J. Comput. Phys. **162**, 429–466 (2000).
25. A. V. Gusarov and I. Smurov, "Gas-dynamic boundary conditions of evaporation and condensation: numerical analysis of the Knudsen layer," Phys. Fluids **14**, 4242–4255 (2002).
26. V. A. Titarev, "Numerical method for computing two-dimensional unsteady rarefied gas flows in arbitrarily shaped domains," Comput. Math. Math. Phys. **49**, 1197–1211 (2009).
27. S. Yoon and A. Jameson, "Lower-upper symmetric Gauss–Seidel method for the Euler and Navier–Stokes equations," AIAA J. **26**, 1025–1026 (1988).
28. I. Men'shov and Y. Nakamura, "An implicit advection upwind splitting scheme for hypersonic air flows in thermochemical nonequilibrium," *Collection of technical papers of 6th Int. Symp. on CFD,* Lake Tahoe, Nevada, 1995, pp. 815–821.
29. M. N. Petrov, A. A. Tambova, V. A. Titarev, S. V. Utyuzhnikov, and A. V. Chikitkin, "FlowModellium software package for calculating high-speed flows of compressible fluid," Comput. Math. Math. Phys. **58**, 1865–1886 (2018).
30. A. Chikitkin, M. Petrov, V. Titarev, and S. Utyuzhnikov, "Parallel versions of implicit LU-SGS method," Special Iss. Lobachevskii J. Math. on Parallel Structure of Algorithms **39**, 503–512 (2018).
31. I. V. Abalakin, P. A. Bakhvalov, A. V. Gorobets, A. P. Duben', and T. K. Kozubskaya, "Parallel software package NOISETTE for large-scale computations of aerodynamical and aeroacoustics problems," Vych. Met. Program. **23** (3), 110–125 (2012).
32. A. V. Gorobets, "Parallel algorithm of the NOISEtte code for CFD and CAA simulations," Lobachevskii J. Math. **39**, 524–532 (2018).
33. V. V. Aristov and S. A. Zabelok, "A deterministic method for solving the Boltzmann equation with parallel computations," Comput. Math. Math. Phys. **42**, 406–418 (2002).
34. V. A. Titarev, Numerical simulation of 3D flows of rarefied gas using a supercomputer, Doctoral Dissertation in Mathematics and Physics (Federal Research Center "Computer Science and Control," Russian Academy of Sciences Moscow, 2018).
35. A. Semin, E. Druzhinin, V. Mironov, A. Shmelev, and A. Moskovsky, "The Performance characterization of the RSC PetaStream module," *29th Int. Conf., ISC 2014,* Leipzig, Lect. Notes Comput. Sci. **8488**, 420–429, (2014).
36. A. J. Lofthouse, "Nonequilibrium hypersonic aerothermodynamics using the direct simulation Monte Carlo and Navier–Stokes models, Ph.D. Thesis (The University of Michigan, 2008).
37. S. Dietrich and I. D. Boyd, "Scalar and parallel optimized implementation of the direct simulation Monte Carlo method," J. Comput. Phys. **126**, 328–342 (1996).
38. A. A. Frolova and V. A. Titarev, "Recent progress on supercomputer modelling of high-speed rarefied gas flows using kinetic equations," Supercomput. Frontiers Innov. **5** (3), 117–121 (2018).
39. A. A. Frolova and V. A. Titarev, "Kinetic methods for solving nonstationary problems with streaming flows," Mat. Mat. Model., No. 4, 27–44 (2018).
40. V. A. Titarev and A. A. Frolova, "Application of model kinetic equations to calculations of super- and hypersonic molecular gas flows," Fluid Dyn. **53**, 536–551 (2018).
41. A. V. Kashkovsky, Ye. A. Bondar, G. A. Zhukova, M. S. Ivanov, and S. F. Gimelshein, "Object-oriented software design of real gas effects for the DSMC method," *24th International Symposium on Rarefied Gas Dynamics,* AIP Conf. Proc. **762**, 583–588 (2004).
42. M. S. Ivanov, A. V. Kashkovsky, S. F. Gimelshein, G. N. Markelov, A. A. Alexeenko, Ye. A. Bondar, G. A. Zhukova, S. B. Nikiforov, and P. V. Vashenkov, "SMILE System for 2D/3D DSMC computations," *Proc. of 25th Int. Symp. on RGD* (Publishing House of the Siberian Branch of the Russian Academy of Sciences, 2007) pp. 539–544.
43. M. Ivanov, A. Kashkovsky, P. Vashchenkov, and Y. Bondar, "Parallel object-oriented software system for DSMC modeling of high-altitude aerothermodynamic problems," *27th Int. Symp. on Rarefied Gas Dynamics,* AIP Conf. Proc. **1333**, 211–218 (2010).
44. G. V. Shoev, Ye. A. Bondar, G. P. Oblapenko, and E. V. Kustova, "Development and testing of a numerical simulation method for thermally nonequilibrium dissociating flows in ANSYS Fluen," Thermophys. Aeromech. **23**, 151–164 (2016).
45. A. A. Shevyrin, Ye. A. Bondar, S. T. Kalashnikov, V. I. Khlybov, and V. G. Degtyar', "Direct simulation of rarefied high-enthalpy flow around the RAM C-II capsule," High Temp. **54**, 383–389 (2016).
46. A. Molchanova, A. Kashkovsky, and Ye. Bondar, "Surface recombination in the direct simulation Monte Carlo method," Phys. Fluids **30**, 107105 (2018).
47. V. A. Titarev, A. A. Frolova, V. A. Rykov, P. V. Vashchenkov, A. A. Shevyrin, and Ye. A. Bondar, "Comparison of the Shakhov kinetic equation and DSMC method as applied to space vehicle aerothermodynamics," J. Comput. Appl. Math. **364**, 1–12 (2020).
48. Vl. Voevodin, A. Antonov, D. Nikitenko, P. Shvets, S. Sobolev, I. Sidorov, K. Stefanov, Vad. Voevodin, and S. Zhumatiy, "Supercomputer Lomonosov-2: Large scale, deep monitoring and fine analytics for the user community," Supercomput. Frontiers Innov. **6** (2), 4–11 (2019).

Translated by A. Klimontovich